ARCHIVES
of
FOUNDRY ENGINEERING

10.24425/afe.2026.157984

Published quarterly as the organ of the Foundry Commission of the Polish Academy of Sciences

ISSN (2299-2944)
Volume 2026
Issue 2/2026

5 – 14

1/2

Comparative Analysis of Fresh and Reclaimed Core Sand in Foundry Reuse Applications

A. Dugu [a, b, *], A. Diószegi [b], J.E. Elfsberg [a, b], B.B. Domeij [a], I. Hollinger [b], M.P. Espinosa [b], T. Nilsson [b], M. Kindstedt [b]
[a] Jönköping University, Sweden
[b] Scania CV AB, Sweden
* Corresponding author: E-mail address: alain.dugu@ju.se

Received 29.10.2025; accepted in revised form 04.02.2026; available online 17.06.2026

Abstract

This study examines chemical composition and grain morphology in fresh and reclaimed silica sand used for core production in an industrial iron foundry. The aim was to characterise in-house core sand before and after dry mechanical reclamation and to assess how repeated use affects element distribution and grain shape. Fresh and reclaimed sand samples from the core sand system were gathered and divided into standard size categories through sieving. The material was subsequently organised into fine, medium, and coarse layers using a stratified approach. X-ray fluorescence (XRF) was used to determine the chemical composition, while dynamic image analysis assessed grain shapes by examining roundness at the Q10, Q50, and Q90 percentiles. Selected samples were additionally examined using scanning electron microscopy (SEM).
Reclaimed sand, especially fine particles (<0.125 mm), has higher levels of MgO, Al_2O_3, CaO, and C than fresh sand due to accumulated bentonite, binder residues, and dust. SiO_2 remains the main component but is slightly lower in reclaimed material due to the higher share of these additional phases. Na_2O decreases slightly in reclaimed sand, while K_2O shows minimal variation between fractions and layers. Grain roundness differs only moderately and depends on size: fresh sand is more rounded in the fine fractions (63 µm and 90 µm), both sands have almost identical roundness in the 125–355 µm range, and reclaimed sand is only slightly more rounded in the coarse fractions (500–710 µm). Scanning electron microscopy (SEM) images indicate that both sand samples exhibit generally similar grain morphologies. However, differences in surface characteristics are likely attributable to a thin coating of fine clay and binder particles present on the reclaimed grains.

Keywords: Foundry sand, Sand reclamation, Mechanical wear, Silica sand, Grain morphology, Chemical composition, Scanning electron microscopy (SEM), X-ray fluorescence (XRF), Stratified sampling

1.Introduction

In foundry operations, casting molds and cores rely heavily on molding sand with consistent properties. Naturally occurring sand often contains a mix of grain sizes and organic materials, necessitating processes such as wet classification and drying to achieve uniform grain distribution. Due to Sweden's limited supply of high-quality quartz sand suitable for foundry use, the majority of the quartz sand used there is imported from natural deposits in other countries [1].

The global casting industry produced approximately 93.5 million tons in 2008, generating an equivalent amount of waste primarily composed of used molding and core sands. These often contain hazardous substances, underlining the importance of efficient sand reclamation methods—especially for silica sand, the primary component, as explained by Dańko et al. [2].

There are two primary techniques utilized: mechanical attrition and thermal reclamation. Mechanical attrition is often chosen due to its cost-effectiveness and its ability to eliminate residual binders from sand grains. All processes lose some sand due to burn-on, spillage, inefficiencies, and dust removal. Overall, total sand loss can reach up to 10%, with about 5% attributed to fine dust.

Additionally, certain inorganic binder systems complicate reclamation efforts due to their lack of burn-on behaviour, as observed by Dańko et al. [3].

Grain size plays a pivotal role in molding sand performance. Coarser, more uniform grains improve permeability and thermal resistance, essential for mold stability. Fine particles occupy intergranular spaces, decreasing permeability but improving surface smoothness [4]. Recognizing this, Scania initiated a project on core sand reclamation despite having no prior experience in the area.

Scania adopted mechanical reclamation, a technology that tends to round off sand grains according to Silva et al. [5]. Throughout this paper, mechanical reclamation refers specifically to a dry mechanical attrition process in a continuous drum-type sand reclaimer, in which the sand is tumbled in a rotating drum and the grains abrade against one another and against the internal liners, with only limited crushing of weak agglomerates. The company aimed to reintegrate 75–80% of reclaimed sand into new sand cores, a significant sustainability milestone. This study investigates the reclamation process by analysing both new and reclaimed sand. Key evaluation methods include XRF for chemical composition, SEM imaging, and laser particle analysis for physical characterization.

The primary aim of this study is to analyse the chemical, structural, and morphological characteristics of the sand before and after mechanical reclamation, specifically in relation to core manufacturing. The core binder system used is a polyurethane cold box (PUCB) epoxy. The green sand mixture also includes binders, bentonite, and carbonaceous additives. During casting, molten iron interacts with the sand, and feeder materials can introduce additional elements, potentially altering the sand's composition.

An important aspect of the reclamation process is the separation of sand used for mold production from that used in cores. Complete separation is difficult due to limitations in the mechanical handling system. Before mechanical attrition begins, a portion of green sand becomes mixed into the core sand stream during the sand recovery process. It is estimated that roughly 30% of the sand in the core stream originates from the mold line. This unintentional mixing introduces variability in the reclaimed core sand, particularly affecting parameters such as grain size, chemical composition, and residual binder content. Understanding this variation is essential for evaluating the quality of reclaimed sand and ensuring reliable core performance.

Figure 1 illustrates the sand processing flow at Scania's foundry. Each hour, the system handles 120 tons of sand: 100 tons from molds and 20 tons from cores. Of this total, 108 tons return to the mold line, and 7 tons are reused for making cores.

Due to the inefficiency of reclaimed sand and its failure to meet foundry quality standards, as well as challenges with separation, approximately 65% of the core sand must be replaced with fresh material. The figure also highlights sand losses at each stage of the process.

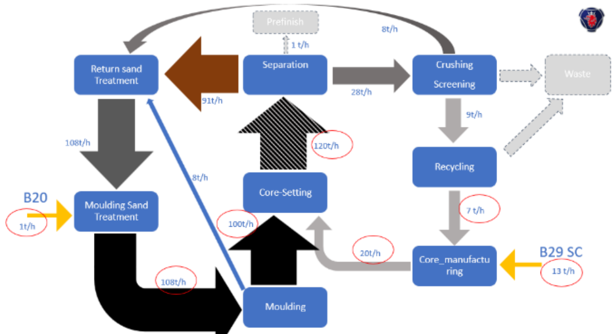

Fig. 1. Sand Processing at Scania Foundry

2. Materials and Method

2.1 Mechanical Reclamation line

This study used sand obtained by a dry mechanical process. The material did not undergo any water exposure or heat processing. The process starts with magnetic separation. After knock-out, the sand passes under a magnetic separator, which removes metallic particles such as shot and small iron pieces. This reduces wear in the downstream equipment and prevents metal from returning to the sand system. Next, the sand is directed to a classifier or screening unit that filters out grains that aren't within the specified size range. Oversized clumps and very coarse grains are eliminated, leaving only sand of the appropriate size to proceed to mechanical reclamation. Mechanical reclamation uses a three-stage drum attrition unit. Inside this rotating drum, sand tumbles as the grains grind against one another and the drum's inner liners. The main processes are abrasion and inter-granular friction, with little crushing of weaker agglomerates. These stages gradually remove the used binder and other loose material from the surface of the grains.

After the drum, the sand passes again through a classifier with cooling. At this point, the sand is cooled, and grains that fall outside the desired size range are separated and removed. During mechanical reclamation, the dust-removal system eliminates fine dust, so that only sand meeting the desired grain-size specifications is sent back into production.

Figure 2 illustrates a simplified version of this process, which includes magnetic separation, classification, three-stage mechanical reclamation, a final classification step, and cooling.

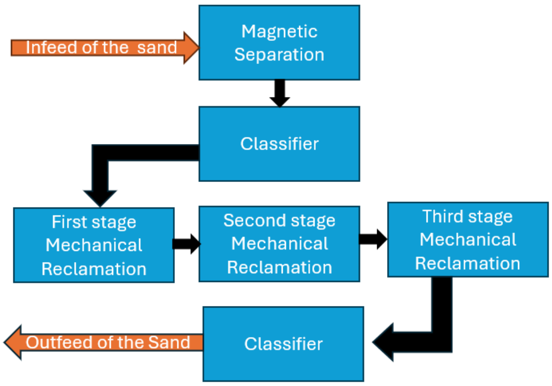

Fig. 2. Simplified schematic of the sand processing and mechanical reclamation line at Scania's foundry

2.2. Moulding and core sand compositions and fresh silica sand

The foundry uses two main sand systems: a green moulding sand for mould production and a polyurethane cold-box (PUCB) core sand for cores. The green moulding sand is based on a silica sand matrix. Per 100 parts by mass of sand grains, the mixture contains about 9 parts bentonite as the main binder, in total around 3–4 parts carbonaceous additives (coal powder, coke and graphite), about 4 parts water and small amounts (each below 1 part) of other mineral components. These values are approximate and indicate the level of binders and additives relative to the sand matrix. The core sand is prepared from fresh silica sand with a PUCB binder system. The core mix contains 100 parts sand, 1 part resin, 1 part hardener, and a small amount of amine gas catalyst. Curing takes place in a core box using an amine gas stream. Routine dry sieve analysis is performed on fresh silica sand, which serves as the base material for both molding and core sands. Table 1 shows the average grain-size distribution, given as the mass percentage remaining on each standard sieve.

Table 1.
Average grain-size distribution of the fresh silica sand used as matrix (n = 91).

Sieve size (mm)	Mean mass retained (%)	Cumulative retained (%)	Cumulative passing (%)
<0.063	0	0	100
0.063	0	0	100
0.090	2	2	98
0.125	13	16	84
0.180	31	47	53
0.250	37	84	16
0.355	13	97	3
0.500	3	100	0
0.710	0	100	0
1.000	0	100	0

The majority of sand is retained on sieves with openings between 0.180 mm and 0.355 mm, with very little material being smaller than 0.063 mm or larger than 0.710 mm. Exhibiting an average grain size of approximately 0.280 mm and an AFS fineness number close to 66, this medium-grade silica sand is particularly appropriate for the castings being evaluated. Because some of the moulding sand is reclaimed and reused in cores, the fresh sand's original composition and grain size directly influence the chemical and physical properties of the reclaimed core sand analysed in this study.

2.3 Theoretical Framework for Obtaining Statistically Representative Sand Data

A stratified sampling method was employed to guarantee that the collected data accurately reflected the entire population. This technique involves dividing the total sample population into subgroups (strata) based on common characteristics. Ensuring that each subgroup is represented in the sample according to its size, as noted by Bornstein et al., leads to more precise statistical estimates. [6]. Cochran [7] provides a more detailed explanation of the idea and statistical basis of this method.

2.3.1 Stratified Sampling Techniques

In stratified sampling, a population of size *N* is divided into *L* distinct, non-overlapping subgroups known as strata. Each stratum has a size denoted by $N_1, N_2, \ldots, N\_L$, so that:

$$N_1+N_2+\ldots+N_L = N \quad [7]$$

Once the strata have been defined, independent samples are drawn from each group. Each group's sample size is denoted by $n_1, n_2, \ldots, n\_L$. Stratified random sampling involves choosing a simple random sample from each individual subgroup, or stratum [7].

2.3.2 Theory of stratified Estimation

Here is how to calculate the stratified estimate of the population mean:

$$\bar{y}st = \frac{\sum_{h=1}^{L} N_h \bar{y}_h}{N} \quad [7]$$

where:
$\bar{y}_{st}$ The symbol represents the sample mean of stratum h, and N_h denotes the population size of stratum h [7].

This estimator ensures that each stratum's contribution is proportionately weighted. When the sampling fractions are identical across all strata (i.e., nh/n = Nh/N), the samples are self-weighting, which streamlines the analysis process. to coincide with the overall sample [7].

2.4 Sample Preparation Method

The mechanical reclamation process used in the facility tends to generate fine particles due to binder abrasion. These fines may retain residual organic or inorganic materials, potentially affecting the performance of sand in core production.

To evaluate this effect, both fresh and reclaimed sand samples were sorted into ten standard grain size ranges: less than 0.063 mm, 0.063 mm, 0.090 mm, 0.125 mm, 0.180 mm, 0.250 mm, 0.355 mm, 0.500 mm, 0.710 mm, and 1.000 mm.

After sieving, both fresh and reclaimed sand were separated into ten standard size fractions (<0.063 mm to 1.000 mm). In practice, two fractions were not available in measurable amounts (0.710 mm and 1.000 mm), so no analysis was carried out for these sizes. The remaining eight fractions were analysed. The fractions were also grouped into three size classes (fine, medium, and coarse) for comparison. Figure 3 shows the three size classes, and Figure 4 shows the analysed sieve fractions.

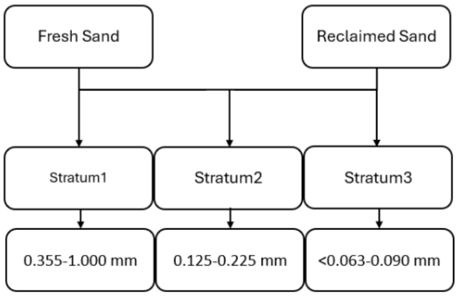

Fig. 3. Samples, categorised into three strata

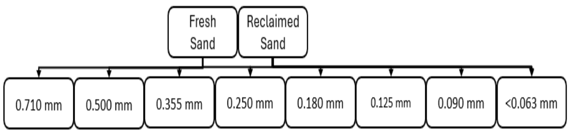

Fig. 4. Samples divided into eight analysed sieve fractions; the less than 0.063 mm and 1.000 mm fractions were not analysed because the sieving produced no measurable retained material

2.5. Sand Characterization by Morphology and chemical composition

A dynamic image analysis system measured both the shapes and sizes of sand grains found in the samples. This method provides detailed data on particle form and dimensions by capturing two-dimensional images of individual grains. A dry dispersion unit distributed particles evenly with compressed air during measurement. To ensure a steady flow of samples during analysis, a vibratory feeder and a rotating plate were employed. The system covers a particle size range from 0.1 µm to 875 µm and is suitable for both fine and coarse sand fractions, allowing reliable analysis of powders, including cohesive or irregularly shaped particles, as described in the Sympatec documentation [8].

The roundness of the sand particles was indicated by their percentile values.

- SD. Q (10) refers to the roundness value below which 10% of the particles fall. It represents the least rounded, most angular grains.
- SD. Q (50) is the median roundness value. Half of the particles in the sample have a roundness lower than this value, and half higher.
- SD. Q (90) shows the roundness value below which 90% of particles fall, highlighting the most rounded grains in the sample.

The dynamic image analysis software automatically determined the shape descriptors from the captured images, and these measurements were obtained directly from the software. Roundness is measured as a percentage, with 100% representing a particle that is perfectly round[8].

X-ray fluorescence (XRF) was also employed to determine the chemical composition of the sand. This technique determines element concentrations without causing damage by detecting the unique X-rays each element emits. The method accounts for matrix effects and background signals to improve accuracy. Careful sample preparation and improved calibration methods helped reduce both systematic and random errors. Results reflect actual elemental levels rather than instrument detection limits, following procedures described by Rousseau et al [9].

3. Results

3.1. Elemental Composition Trends Across Sand Types

Table 2 presents the chemical composition of the materials used to produce the final molding sand. These materials include two types of binders and dust collected from the production process. Each component's elemental makeup was determined using X-ray fluorescence (XRF) analysis.

Additives are combined with reclaimed sand to alter its properties, producing the molding sand required for casting. The final column in Table 2 shows the overall chemical composition of the resulting molding sand after mixing.

This analysis is important because about 30% of the molding sand is ultimately recovered and reused when making cores. As a result, the chemical composition of the original molding sand can significantly influence the reclaimed core sand. Understanding the contribution of each additive helps to explain how specific elements may persist or change during the reclamation process.

Table 2.
Chemical Composition of Binders, Production Dust, and Resulting Molding sand

Compounds	Low-carbon bentonite	Higher-carbon bentonite	Dust from production	Mold sand
C	9,10%	13,82%	10,68%	1,24%
Moisture	6,71%	7,66%	2,10%	0,24%
CaO	3,46%	3,42%	3,00%	0,36%
MgO	3,51%	3,55%	2,24%	0,19%
SiO_2	61,80%	61,60%	68,00%	82,70%
Al_2O_3	20,00%	20,00%	17,40%	10,60%
MnO	0,05%	0,05%	0,04%	0,02%
Cr_2O_3	<0,01%	0,00%	0,01%	0,03%
V_2O_5	2,00%	0,02%	0,01%	<0,01%
TiO_2	0,86%	0,83%	0,48%	0,08%
Na_2O	2,27%	2,46%	2,26%	0,91%
K_2O	0,88%	0,89%	2,31%	3,32%
P_2O_5	0,13%	0,11%	0,15%	0,05%
SO_3	1,39%	1,25%	1,13%	0,10%
Fe_2O_3	5,49%	5,79%	2,96%	1,54%
ZnO	0,10%	0,01%	< 0,01 %	>0,01
CuO	1,00%	0,00%	0,00%	0,01%
SrO	0,02%	<0,01 %	< 0,01 %	< 0,01 %
BaO	0,06%	0,05%	0,05%	0,10%

Table 3 presents the chemical composition of sand used in core production, as determined by XRF analysis.
This analysis examines two types of sand: fresh sand, which is newly introduced into the process, and reclaimed sand, which has undergone reclamation procedures for subsequent reuse. This analysis delineates the compositional differences between fresh and reclaimed sand, offering a detailed assessment of the alterations resulting from the reclamation process.

Table 4 presents the chemical composition of both fresh and reclaimed sand, categorized into three different grain-size strata: Stratum 1, Stratum 2, and Stratum 3. The values are again based on XRF measurements. The carbon content and various oxides present in the strata vary according to the proportion of fine and coarse grains in each group

Table 3.
Comparative Chemical Composition of Fresh and Reclaimed Sand for Core Production

Compounds	Fresh Sand	Reclaimed sand
MgO	0,04%	0,14%
Cr_2O_3	0,02%	0,03%
TiO_2	0,06%	0,09%
BaO	0,05%	0,06%
Al_2O_3	6,39%	6,54%
CaO	0,36%	0,37%
Na_2O	1,21%	1,15%
K_2O	2,89%	2,89%
MnO	0,01%	0,01%
ZrO_2	0,01%	0,01%
SiO_2	88,30%	87,50%
Fe_2O_3	0,62%	0,54%
SrO	0,01%	0,00%

Table 4.
Chemical Composition of Stratified Sand Samples

Compounds	Fresh Sand			Reclaimed Sand		
	Stratum1	Stratum2	Stratum3	Stratum1	Stratum2	Stratum3
C	0,01%	0,00%	0,01%	0,32%	0,70%	1,08%
Moisture	0,05%	0,04%	0,05%	0,08%	0,00%	0,23%
CaO	0,33%	0,34%	1,29%	0,32%	0,45%	1,57%
MgO	0,12%	0,07%	0,22%	0,12%	0,17%	0,46%
SiO_2	86,30%	87,00%	80,20%	87,20%	87,40%	79,10%
Al_2O_3	7,39%	6,94%	9,08%	6,97%	6,84%	10,20%
MnO	<0,01%	0,00%	0,06%	<0,01%	<0,01%	0,04%
Cr_2O_3	0,01%	0,03%	0,03%	0,03%	0,03%	0,02%
V_2O_5	0,00%	0,00%	<0,01%	0,00%	0,00%	<0,01%
TiO_2	0,05%	0,05%	0,61%	0,05%	0,06%	0,50%
Na_2O	1,34%	1,32%	1,83%	1,18%	1,22%	1,83%
K_2O	3,90%	3,66%	3,87%	3,49%	3,10%	3,93%
P_2O_5	0,03%	0,00%	0,18%	0,04%	0,06%	0,15%
SO_3	0,00%	0,00%	0,00%	0,03%	0,08%	0,16%
Fe_2O_3	0,44%	0,49%	2,36%	0,50%	0,57%	1,82%
ZnO	0,00%	0,00%	0,00%	0,00%	0,00%	0,11%

Table 5 and Table 6 present the composition of sand separated into individual sieve fractions for fresh sand (Table 5) and reclaimed sand (Table 6). Each fraction contains specific amounts of carbon, moisture, and oxides, making it possible to closely compare different grain sizes as well as fresh versus reclaimed material.

Table 5.
Chemical Composition of Particle Size Fractions in Sample (100% fresh sand)

Compounds	Sample 1								
	0,710 mm	0,500 mm	0,355 mm	0,250 mm	0,180 mm	0,125 mm	0,090 mm	0,063 mm	<0,063 mm
C	0,01%	0,02%	<0,002%	<0,002%	0,00%	0,00%	0,00%	0,02%	0,04%
Moisture	0,04%	0,00%	0,04%	0,10%	0,00%	0,05%	0,05%	0,19%	0,00%
CaO	0,69%	0,36%	0,28%	0,22%	0,34%	0,67%	0,74%	2,52%	1,62%
MgO	0,14%	0,08%	0,06%	<0,01%	0,04%	0,15%	0,15%	0,51%	0,29%
SiO_2	81,30%	88,20%	87,30%	90,00%	87,20%	85,40%	85,30%	71,00%	73,60%
Al_2O_3	10,30%	6,30%	6,87%	5,52%	7,15%	7,75%	7,42%	9,90%	10,80%
MnO	< 0,01 %	0,01%	0,00%	0,00%	< 0,01 %	0,01%	0,02%	0,11%	0,06%
Cr_2O_3	0,03%	0,02%	0,02%	0,04%	0,02%	0,01%	0,03%	0,01%	0,04%
V_2O_5	0,00%	0,00%	0,00%	0,00%	0,00%	< 0,01 %	0,00%	0,02%	0,00%
TiO_2	0,07%	0,05%	0,04%	0,04%	0,05%	0,16%	0,21%	1,67%	1,11%
Na_2O	2,19%	1,13%	1,17%	1,00%	1,38%	1,45%	1,40%	1,94%	2,00%
K_2O	4,34%	3,26%	3,68%	2,68%	3,32%	3,55%	3,58%	4,00%	4,53%
P_2O_5	0,04%	0,03%	0,00%	0,02%	0,00%	0,05%	0,10%	0,62%	0,37%
Fe_2O_3	0,88%	0,53%	0,43%	0,44%	0,39%	0,74%	1,00%	6,73%	4,75%
SrO	< 0,01 %	< 0,01 %	< 0,01 %	< 0,01 %	< 0,01 %	< 0,01 %	0,01%	< 0,01 %	< 0,01 %
BaO	0,10%	0,06%	0,09%	0,06%	0,06%	0,05%	0,06%	0,03%	0,09%
ZrO_2	0,00%	0,00%	0,00%	0,00%	0,00%	0,00%	0,02%	0,71%	0,54%
HfO_2	0,00%	0,00%	0,00%	0,00%	0,00%	0,00%	0,00%	0,22%	0,19%

Table 6.
Chemical Composition of Particle Size Fractions in Sample 5(100% reclaimed sand)

	Sample 5								
Compounds	0,710 mm	0,500 mm	0,355 mm	0,250 mm	0,180 mm	0,125 mm	0,090 mm	0,063 mm	<0,063 mm
C	0,41%	0,33%	0,38%	0,46%	0,68%	0,95%	1,08%	1,25%	1,62%
Moisture	0,00%	0,00%	0,10%	0,05%	0,00%	0,05%	0,52%	0,25%	0,35%
CaO	0,69%	0,45%	0,28%	0,33%	0,39%	0,73%	1,24%	1,37%	0,35%
MgO	0,24%	0,14%	0,06%	0,14%	0,18%	0,29%	0,40%	0,36%	0,10%
SiO_2	80,30%	86,70%	87,70%	88,00%	86,70%	82,80%	79,90%	75,60%	86,40%
Al_2O_3	11,10%	7,19%	6,79%	6,31%	7,41%	9,38%	10,70%	11,90%	7,42%
MnO	0,01%	< 0,01 %	< 0,01 %	< 0,01 %	< 0,01 %	0,01%	0,03%	0,06%	< 0,01 %
Cr_2O_3	0,03%	0,03%	0,03%	0,02%	0,03%	0,01%	0,04%	0,03%	0,02%
TiO_2	0,11%	0,04%	0,04%	0,05%	0,09%	0,13%	0,30%	0,55%	0,04%
Na_2O	1,95%	1,18%	1,04%	1,10%	1,35%	1,60%	1,72%	1,82%	1,31%
K_2O	4,52%	3,46%	3,54%	3,35%	3,19%	4,00%	3,89%	4,82%	3,73%
P_2O_5	0,03%	0,03%	0,00%	0,04%	0,00%	0,08%	0,14%	0,19%	0,00%
SO_3	0,05%	0,05%	0,01%	0,06%	0,06%	0,11%	0,11%	0,26%	0,00%
Fe_2O_3	0,83%	0,59%	0,48%	0,49%	0,57%	0,82%	1,33%	2,53%	0,49%
SrO	< 0,01 %	< 0,01 %	< 0,01 %	< 0,01 %	< 0,01 %	0,01%	< 0,01 %	< 0,01 %	0,01%
BaO	0,13%	0,11%	0,07%	0,05%	0,06%	0,07%	0,10%	0,16%	0,10%
Cl	< 0,01 %	0,00%	0,00%	0,00%	0,00%	0,00%	0,02%	0,00%	0,00%
ZrO_2	0,00%	0,00%	0,00%	0,00%	0,00%	0,00%	0,03%	0,27%	0,00%
HfO_2	0,00%	0,00%	0,00%	0,00%	0,00%	0,00%	0,00%	0,06%	0,00%

3.2. Morphological Characteristics of Fresh vs. Reclaimed Sands

3.2.1 Roundness of fresh and reclaimed sand

Figures 5 to 7 show the roundness of sand grains in fresh and reclaimed sand across various sieve size fractions. Roundness is reported using three values, each based on percentiles obtained from image analysis.

SD. Q (10) reflects the least rounded 10% of grains, indicating the more angular portion of the sample.
SD. Q (50) represents the median roundness.
SD. Q (90) indicates the most rounded 10% of grains in each sample.

The roundness of a particle is expressed as a percentage, where 100% means the particle is perfectly rounded.
The graphs present the data separately for each roundness percentile:

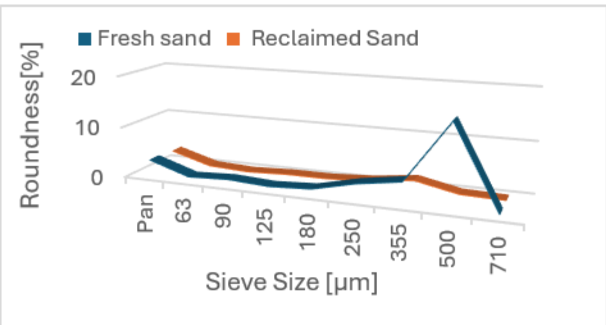

Fig. 5. Roundness (Q10) of Fresh and Reclaimed Sand by Grain Size Fraction

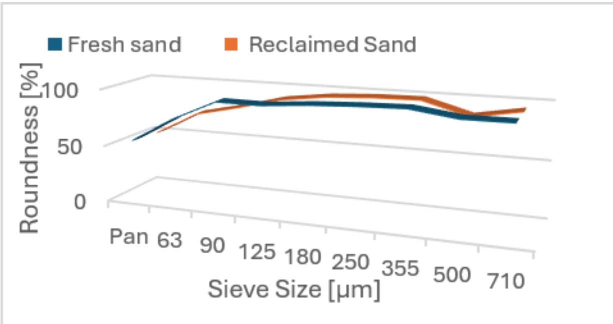

Fig. 6. Roundness (Q50) Percentile by Grain Size in Fresh Sand

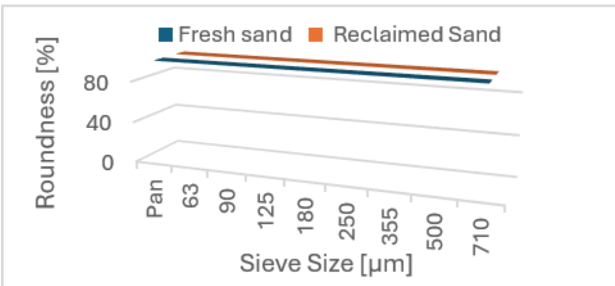

Fig. 7. Roundness (Q90) Distribution across Core Sand Fractions

3.2.2 Surface Morphology of Sand Grains: SEM Observations

Figure 5 displays both scanning electron microscope (SEM) and macroscopic images used to document the morphology of fresh and reclaimed sand. The top row shows SEM images of the sand samples, where the left image corresponds to fresh sand and the right to reclaimed sand.

These SEM images, taken at the same magnification, display the fine-scale grain structure and surface texture. The bottom row presents macroscopic photographs of the same sample types. The image on the left shows fresh sand, while the image on the right shows reclaimed sand. These photographs illustrate overall grain colour, shape, and surface appearance observable to the naked eye. All images serve as a visual record of the physical condition of the sand before and after the reclamation process.

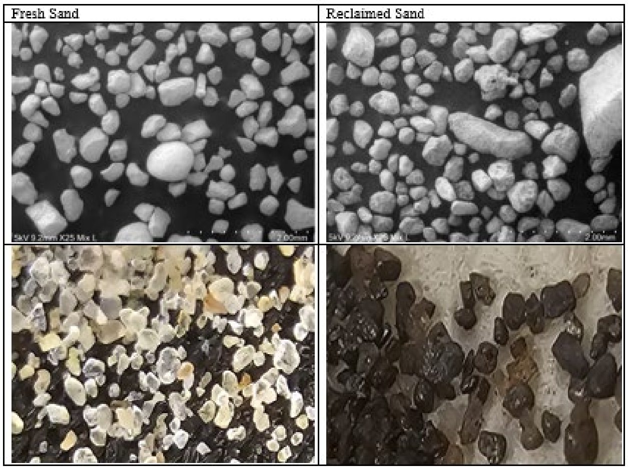

Fig. 8. SEM and Macroscopic Images Showing Grain Surface of Fresh and Reclaimed Sand

4. Discussion from the Result

4.1. Elemental Composition Trends Across Sand Types

Mechanical reclamation works through attrition, where sand grains rub against each other and against machine surfaces to clean their outer layers. Khan et al. [10] found that this method reduces loosely bound dead clay in waste sand from around 10% to 2.2%, though it cannot remove binders trapped in grain cracks or oolitic layers. Svoboda [12] noted that mechanical reclamation consistently generates dust, and even after multiple cycles, some fine binder residues still remain in the reclaimed sand.

The chemical analysis of fresh and reclaimed foundry sand shows key changes in composition resulting from the reclamation process. After undergoing mechanical treatment to eliminate binders and impurities, reclaimed sand is recycled for further use; however, it may retain trace residues from its previous applications. One notable change is the increase in magnesium oxide, which rises from 0.04% in fresh sand to 0.14% in fully reclaimed sand. The increase is mainly due to residual bentonite, particularly where fine clay particles gather. Bentonite—typically Na,Ca)0.33$(Al,Mg)_2(Si_4O_{10})(OH)_2 \cdot nH_2O$—contains magnesium in its layered montmorillonite structure[11].

Aluminium oxide increases from 6.39% in fresh sand to over 10% in reclaimed sand, likely because of bentonite. This rise is most noticeable in the finer grain fractions, suggesting that clay residues are difficult to remove by mechanical or thermal reclamation. Mechanical scrubbing has difficulty removing the tiny clay particles because they cling tightly to the sand grains. Svoboda [12] reports that mechanical reclamation recovers 75–90% of usable sand but generates significant dust, making fine particle separation difficult. Fresh sand contains little carbon, while reclaimed sand—especially finer particles—can have over 1.6%. The main reason for the increase is that some binder materials and additives remain after reclamation and are not completely removed. Carbon residues accumulate as small, hard-to-clean particles. Łucarz et al. [13] confirmed that carbon residues can persist even after thermal treatment, showing their resistance to standard reclamation.

Calcium oxide (CaO) shows a moderate increase in reclaimed sand, with the highest concentrations often found in the finer fractions. The rise is probably due to leftover calcium additives and dust from molding. Fine particles tend to retain these residues more easily, leading to their build-up in the smaller grain sizes of reclaimed sand. Dańko et al. [14] reported that dust collected after mechanical reclamation contains elevated calcium levels, confirming that fine particles retain calcium-bearing compounds that are difficult to remove.

Titanium dioxide (TiO_2) shows a slight increase in reclaimed sand, especially in coarse grains. According to Górny et al. [15], titanium is deliberately introduced into compacted graphite iron to improve and refine its microstructure. During casting, some titanium can remain in the mold, becoming embedded in the sand. Jung et al. [16] noted that titanium is also present in ladle slags as titanium oxide, which may play a role in this enrichment process.

Iron oxide content decreased from 0.62% to 0.54%, probably due to partial magnetic separation during reclamation. Jonczy et al.[17] observed that reclaimed sand contains magnetite, hematite, and wüstite, as well as trace amounts of metallic iron, which explains the low residual concentrations detected.

There are only minor variations in sodium oxide and potassium oxide content between fresh and reclaimed sand. Na_2O is slightly lower in the reclaimed material in the bulk samples and in most grain-size strata, while K_2O changes only within a narrow range between fractions and strata, without a clear overall trend. Yang et al. [18] observe that sodium bentonite affects how different components are distributed in systems containing many fine particles. In the same way, this study presumes that clay containing sodium is likewise redistributed among the finer particle fractions.

Silicon dioxide remains the dominant component in all samples. In bulk sand, SiO_2 decreases slightly from 88.3 % in fresh sand to 87.2 % in reclaimed sand. This relative decrease reflects the higher shares of MgO, Al_2O_3, CaO and C in the reclaimed material, especially in the fine fractions. Jusnes [19] showed that thermal exposure can change the phase state of quartz in industrial sands, but in the present case the main effect is the enrichment of non-silica components rather than a large loss of quartz itself.

4.2. Morphological Characteristics of Fresh vs. Reclaimed Sands

Mechanical reclamation relies on particles rubbing against each other and machine surfaces, which often leads to increased grain roundness, as demonstrated by Silva et al. [5]. At a particle size of 63 µm, fresh sand exhibits approximately 3.7% greater roundness compared to reclaimed sand; at 90 µm, the difference increases to

9.2%. The pan fraction also shows slightly higher roundness in fresh sand (≈ 1.7 %).

In the 125–355 µm range, fresh and reclaimed sands have nearly identical roundness, differing by less than 1%. This indicates that grains in this range keep their shape during the process. Jan et al. [20] pointed out that process conditions and reuse cycles can influence the behaviour of granular materials, and Pettijohn et al. [21] showed that natural transport mechanisms, such as water movement, tend to smooth grains over long distances. Schumacher et al. [22] found that medium sand grains are usually more stable and less prone to breaking or deforming during casting.

In the larger grain sizes of 500 µm and 710 µm, reclaimed sand is just a bit rounder than fresh sand, showing Q50 differences of roughly 0.26–0.45%. This is consistent with gradual smoothing of large grains under repeated collisions and abrasion. Attal and Lavé [23] showed that large particles can abrade slowly but steadily during repeated transport, which leads to more rounded forms over time.

4.3. Surface Morphology of Sand Grains: SEM Observations

SEM images (Figure 8) compare the micro- and macroscopic morphology of fresh and reclaimed samples. Grains appear as mixtures of rounded and angular forms typical of silica-based green-sand systems, as discussed by Altunyurt [24].

SEM images reveal that, at the given magnification, both reference and reclaimed sands consist of irregularly shaped grains with relatively simple outlines. From these images alone, it is not possible to tell whether the observed changes come only from abrasion or also from charging effects. In dry mechanical reclamation, grains continually make contact, collide, and slide with each other as well as with clay or oxide films attached to them—closely resembling the charging process in triboelectric mineral separation systems [25]. In foundry work, triboelectric charging helps explain why velour-like surface layers form: dust generated during reclamation is drawn to the grain surfaces and held there by electrostatic forces.

Previous studies have demonstrated that reclamation processes may effectively clean the surface of grains; however, these procedures typically do not result in notable changes to grain morphology unless the treatment is either particularly aggressive or conducted over multiple cycles, as supported by the findings of M. Lucarz [26].

Overall, the SEM images suggest that mechanical reclamation does not strongly affect grain shape for most particles. Minor signs of wear or small chips along the edges may appear, especially in finer or more delicate grains, though such imperfections are typically very slight.

5. Conclusions

The comparative analysis of fresh and reclaimed foundry sands shows measurable differences in chemical composition and limited, size-dependent differences in grain morphology. Elemental analysis indicates a consistent increase in MgO, Al_2O_3, CaO and C in reclaimed sand, with the highest values in particles smaller than 0.125 mm. The increases are caused by leftover bentonite, binder residues, and fine dust that mechanical reclamation does not completely remove. SiO_2 remains the dominant component in all samples, but its proportion in reclaimed sand is slightly lower than in fresh sand because the relative amounts of MgO, Al_2O_3, CaO and C are higher in the fine fractions.

The levels of sodium oxide and potassium oxide are nearly the same in both fresh sand and reclaimed sand. Na_2O is slightly lower in the reclaimed material in the bulk samples and in most grain-size strata, while K_2O varies only within a narrow range between fractions and strata.

The formation, movement, and partial removal of fine particles that contain sodium- and potassium-bearing phases during sand handling, reclamation, and dust separation are responsible for these changes.

In terms of particle shape, the observed changes are small and clearly dependent on grain size. In the fine fractions of 63 µm and 90 µm, fresh sand is more rounded than reclaimed sand by about 3.7 % and 9.2 % in Q50, respectively, and the pan fraction (< 0.063 mm) also shows slightly higher roundness in fresh sand, by about 1.7 %. This indicates that the fine part of the reclaimed sand contains more newly formed, irregular fragments that arise from the break-up of larger grains during pneumatic transport, mixing, moulding, knocking out and mechanical reclamation. Fresh and reclaimed sands sized 125–355 µm differ in roundness by under 1%, showing these grains remain mechanically stable after reuse. For the 500 µm and 710 µm fractions, reclaimed sand exhibits only a marginal increase in roundness compared to fresh sand, with Q50 differences reaching up to 0.45%. This suggests that repeated abrasion results in minimal smoothing of larger grain sizes. Overall, these roundness differences do not indicate a major change in the general morphological character of the sand.

SEM observations at low magnification show that the overall grain morphology of fresh and reclaimed sands is similar, with both materials containing mixtures of angular and rounded grains typical of silica-based moulding systems. Within the magnification used, no considerable change in general grain shape is visible. The unique look of some reclaimed grains is mainly due to a thin layer of fine particles sticking to their surfaces. This coating develops when fine particles of clay and binder dust, produced by abrasion, stick to the grain surfaces through both electrostatic and mechanical forces—especially when sodium- and potassium-containing substances are present. If a significant portion of reclaimed sand is used during core production, the grains' effective surface area increases, which means additional binder is needed to adequately coat them. This can lead to a small rise in binder demand. In summary, repeated use and mechanical reclamation chiefly increase the concentration of bentonite and binder components in fine particles, while only causing minor changes in grain roundness between particle sizes.

References

[1] Metallkompetens. (2024). *Sander för formar och kärnor - Metallkompetens*. Retrieved April 4, 2024, from https://metallkompetens.se/handbok/gjuterihandboken/form-

och-karnmaterial-for-engangsformar/sander-for-formar-och-karnor/.
[2] Dańko, R., Dańko, J.S., Holtzer, M. (2010). *Foundry sand reclamation - theory and industrial practice*. Kraków: AGH University of Science and Technology.
[3] Dańko, R., Holtzer, M. & Dańko, J. (2015). Investigations of physicochemical properties and thermal utilisation of dusts generated in the mechanical reclamation process of spent moulding sands. *Archives of Metallurgy and Materials*. 60(1), 313-318. DOI: 10.1515/amm-2015-0051.
[4] Beeley, P. (2001). *Foundry Technology (2nd ed.)*. Oxford: Butterworth-Heinemann.
[5] Silva, E.C., Masiero, I. & Guesser W.L. (2020). Comparing sands from different reclamation processes for use in the core room of cylinder heads and cylinder blocks production. *International Journal of Metalcasting*. 14(3), 706-716. https://doi.org/10.1007/s40962-019-00400-6.
[6] Bornstein, M.H., Jager, J. & Putnick D.L. (2013). Sampling in developmental science: Situations, shortcomings, solutions, and standards. *Developmental Review*. 33, 357-370. DOI: 10.1016/j.dr.2013.08.003.
[7] Cochran, W.G. (1977*). Sampling Techniques (3rd ed.)*. Wiley.
[8] Sympatec. (2024). *Configuration: HELOS-BR-RODOS-VIBRI*. Retrieved April 9, 2024, from https://www.sympatec.com/en/particle-measurement/sensors/laser-diffraction/helos/helos-br-rodos-vibri/.
[9] Rousseau, R.M., Richard, D.R., Rousseau, M. (2014). *Detection limit and estimate of uncertainty of analytical XRF results*. Retrieved January 20, 2026, from https://www.researchgate.net/publication/228687395.
[10] Khan, M. M., Mahajani, S. M., Jadhav, G. N., Vishwakarma, R., Malgaonkar, V. & Mandre, S. (2021). Mechanical and thermal methods for reclamation of waste foundry sand. *Journal of Environmental Management*. 279, 111628, 1-10. https://doi.org/10.1016/j.jenvman.2020.111628.
[11] Karakaya, M.Ç., Karakaya, N. & Küpeli, Ş. (2011). Mineralogical and geochemical properties of the Na- and Ca-bentonites of Ordu (NE Turkey). *Clays and Clay Minerals*. 59(1), 75-94. https://doi.org/10.1346/CCMN.2011.0590109.
[12] Svoboda, J.M. (1990). *Foundry sand reclamation: an overview of foundry mold making operations and a review of sand reclamation methods including emerging electrotechnologies*. CMP Report No. 90-6.
[13] Łucarz, M., Garbacz-Klempka, A., Drożyński, D., Skrzyński, M. & Kostrzewa, K. (2023). Mechanical reclamation of spent moulding sand on chromite sand matrix; removal of alkali-phenolic binder. *Materials (Basel)*. 16(7), 2919, 1-29. https://doi.org/10.3390/ma16072919.
[14] Dańko, R., Jezierski, J. & Holtzer, M. (2016). Physical and chemical characteristics of after-reclamation dust from used sand moulds. *Arabian Journal of Geosciences*. 9(2), 1-8. https://doi.org/10.1007/s12517-015-2162-3.
[15] Górny, M. & Kawalec, M. (2013). Effects of titanium addition on microstructure and mechanical properties of thin-walled compacted graphite iron castings. *Journal of Materials Engineering and Performance*. 22 (5), 1519-1524. https://doi.org/10.1007/s11665-012-0432-8.
[16] Jung, S.-M. & Fruehan, R.J. (2001). Thermodynamics of titanium oxide in ladle slags. *ISIJ International*. 41(12), 1447-1453. https://doi.org/10.2355/isijinternational.41.1447.
[17] Jonczy, I., Kamińska, M., Bilewska, K. & Gerle, A. (2018). Crystalline phases in the waste foundry sands based on quartz sand matrix. *Inżynieria Ochrony Środowiska*. 21(3), 213-226. DOI: 10.17512/ios.2018.3.1.
[18] Xiao, Y., Li, Y., Ning, Z., Li, P., Yang, P., Liu, C., Liu, Z., Xu, F. & Hynds, P. D. (2018). Organic contaminant removal efficiency of sodium bentonite/clay (BC) mixtures in high permeability regions utilizing reclaimed wastewater: A meso-scale study. *Journal of Contaminant Hydrology*. 210, 1-14. https://doi.org/10.1016/j.jconhyd.2018.01.008.
[19] Jusnes, K.F. (2020). *Phase transformations and thermal degradation in industrial quartz*. Retrieved April 22, 2025, from https://ntnuopen.ntnu.no/ntnu-xmlui/handle/11250/2675473.
[20] Jan, R., Diego, G. G., Sergio, G. G. & Manuel, G. G. (2021). A Novel Methodology for Assessing and Modeling Manufacturing Processes: A Case Study for the Metallurgical Industry. In *International Conference on Intelligent Human Computer Interaction* (pp. 184-197). Cham: Springer International Publishing.
[21] Pettijohn, F.J., Potter, P.E., Siever, R. (2012). *Sand and Sandstone.* Springer Science & Business Media.
[22] Wang, X. (2014). *Thermal physical and mechanical properties of raw sands and sand cores for aluminum casting*. Master's Thesis, Montanuniversität Leoben. Leoben.
[23] Attal, M. & Lavé, J. (2009). Pebble abrasion during fluvial transport: Experimental results and implications for the evolution of the sediment load along rivers. *Journal of Geophysical Research: Earth Surface*. 114(F4), F04023, 1-22. https://doi.org/10.1029/2009JF001328.
[24] Altunyurt, A. (2025). *Silica sand: foundry requirements and classification*. Retrieved April 25, 2025, from https://www.academia.edu/19130829/SILICA_SAND_FOUNDRY_REQUIREMENTS_AND_CLASSIFICATION.
[25] Zhao, R., Zhang, Z., Bai, X., Wang, H., Zhang, H., Hao, J. & Wang, C. (2024). A review of the research on triboelectric separation technology. *Minerals Engineering*. 216, 108901, 1-17. https://doi.org/10.1016/j.mineng.2024.108901.
[26] Łucarz, M. (2008). The effect of mechanical reclamation on the wear of silica sand grains. *Metalurgija*. 47 (1), 43-45.